



## OPEN Two *Paenibacillus* spp. strains promote grapevine wood degradation by the fungus *Fomitiporia mediterranea*: from degradation experiments to genome analyses

Rana Haidar<sup>1,2,5</sup>✉, Stéphane Compant<sup>3,5</sup>, Coralie Robert<sup>4,5</sup>, Livio Antonielli<sup>3</sup>, Amira Yacoub<sup>1,2</sup>, Axelle Grélard<sup>4</sup>, Antoine Loquet<sup>4</sup>, Günter Brader<sup>3</sup>, Rémy Guyoneaud<sup>1</sup>, Eléonore Attard<sup>1</sup> & Patrice Rey<sup>1,2</sup>

Ascomycetes, basidiomycetes and deuteromycetes can degrade wood, but less attention has been paid to basidiomycetes involved in Esca, a major Grapevine Trunk Disease. Using a wood sawdust microcosm system, we compared the wood degradation of three grapevine cultivars inoculated with *Fomitiporia mediterranea* M. Fisch, a basidiomycete responsible for white-rot development and involved in Esca disease. The grapevine cultivar Ugni blanc was more susceptible to wood degradation caused by *F. mediterranea* than the cultivars Cabernet Sauvignon and Merlot. Solid-state Nuclear Magnetic Resonance (NMR) spectroscopy showed that *F. mediterranea* preferentially degrades lignin and hemicellulose over cellulose (preferential, successive or sequential white-rot). In addition, co-inoculation of sawdust with two cellulolytic and xylanolytic bacterial strains of *Paenibacillus* (Nakamura) Ash (*Paenibacillus* sp. (S231-2) and *P. amylolyticus* (S293)), enhanced *F. mediterranea* ability to degrade Ugni blanc. The NMR data further showed that the increase in Ugni blanc sawdust degradation products was greater when bacteria and fungi were inoculated together. We also demonstrated that these two bacterial strains could degrade the wood components of Ugni blanc sawdust. Genome analysis of these bacterial strains revealed numerous genes predicted to be involved in cellulose, hemicellulose, and lignin degradation, as well as several other genes related to bacteria-fungi interactions and endophytism inside the plant. The occurrence of this type of bacteria-fungus interaction could explain, at least in part, why necrosis develops extensively in certain grapevine varieties such as Ugni blanc.

The development of grapevine trunk disease (GTD) has become a subject of utmost importance in international viticulture since the 2000s<sup>1,2</sup>. GTDs are associated with wood degradation and the development of various types of wood necrosis. Generally, studies on microbial wood decomposition have suggested that fungi are the main decomposers because of their ability to produce many enzymes involved in lignin, cellulose, and hemicellulose degradation, which destroy wood biopolymers<sup>3-5</sup>. Pathogenic fungi are usually reported as the key microorganisms that degrade grapevine wood in Esca, which is the most widespread GTD worldwide. They are responsible for the discoloration of wood and the development of white-rot necrosis, a final structure in wood degradation, and the most typical symptom of Esca disease<sup>1,2,6,7</sup> also called “amadou” in French. *Fomitiporia mediterranea*

<sup>1</sup>E2S UPPA, CNRS, IPREM UMR5254, Université de Pau et des Pays de l'Adour, Pau, France. <sup>2</sup>INRAE, UMR1065 Santé et Agroécologie du Vignoble (SAVE), ISVV, 33883 Villenave d'Ornon, France. <sup>3</sup>Bioresources Unit, Center for Health and Bioresources, AIT Austrian Institute of Technology GmbH, Konrad Lorenz Straße 24, 3430 Tulln, Austria. <sup>4</sup>Institut de Chimie et Biologie des Membranes et des Nanoobjets, IECB, CNRS, Université de Bordeaux, 33607 Pessac, France. <sup>5</sup>These authors contributed equally: Rana Haidar, Stéphane Compant and Coralie Robert. ✉email: Rana.haidar@univ-pau.fr

is the main white-rotting basidiomycete of grapevine in Europe and the Mediterranean regions. This fungus with a high ligninolytic activity, can degrade grapevine wood tissues and is usually involved in Esca disease<sup>8–10</sup>.

Over the last decade, it has been shown that fungi are not the only microorganisms that colonize grapevine wood tissues, and the occurrence of bacteria in these tissues has been reported in several studies<sup>11–14</sup>. Although certain bacteria could contribute to decay in various plants, including wheat, rice, corn, soybean, and grapevine<sup>15,16</sup>, they have a limited ability to decompose wood components<sup>17,18</sup>. However, it is assumed that the interaction of bacteria with fungi could lead to wood degradation processes<sup>15–21</sup>, and that the synergistic role of bacteria with pathogenic basidiomycetes could increase the degradation of wood components<sup>19,22–24</sup>.

The interactions of bacteria colonizing grapevines with wood-decaying fungi have already been investigated in the context of GTDs. However, most studies have focused on the biocontrol of pathogenic fungi by bacteria<sup>25,26</sup>. Only a few publications<sup>15,27</sup> have investigated the synergistic interactions between these fungi and wood-inhabiting bacteria. For instance, Haidar et al<sup>27</sup> observed an increase in the canker development on grapevine stem cuttings after co-inoculating *Bacillus pumilus* strain S35 and *Xanthomonas* sp. strain S45 with *Neofusicoccum parvum*, a GTD fungus. In addition, it was showed that wood degradation by *F. mediterranea* was enhanced in the presence of a *Paenibacillus* strain identified as a new species of bacteria named *Paenibacillus xylinteritus*<sup>28</sup>. Genome annotation of this last strain revealed the presence of several gene clusters related to carbohydrate-active enzymes, xylose degradation and vitamin metabolism.

To decipher putative interactions between *F. mediterranea* and some bacteria, we: (i) compared the susceptibility of three grapevine cultivars (Cabernet Sauvignon, Merlot, and Ugni blanc) to *F. mediterranea*, and (ii) described the ability of two bacterial strains, *P. amylolyticus* strain S293 and *Paenibacillus* sp. strain S231-2, to enhance wood colonization and decomposition by *F. mediterranea*. The cultivar most sensitive to *F. mediterranea* attack, Ugni blanc, was then selected to study the bacteria-fungus interaction. The two bacterial strains were selected from a previous experiment using wood microcosms (i.e., the medium was made of grapevine sawdust), as they displayed strong cellulase and xylanase activities and did not inhibit the growth of *F. mediterranea* mycelia<sup>15</sup>. However, their role in wood degradation was not determined. Finally, whole genome annotation of the two bacterial strains was performed to determine their potential role to degrade wood components and to produce secondary metabolites that could be involved in bacterial-fungal-plant interactions.

## Results

### Difference in the susceptibility of three grapevine cultivars to *F. mediterranea* attack

#### *F. mediterranea*'s mycelial growth on tested grapevine cultivars wood

Measurement of the mycelial growth of *F. mediterranea* on wood of three cultivars (Cabernet Sauvignon, Merlot, and Ugni blanc) at six and nine days post-inoculation (dpi) revealed that *F. mediterranea* development depended on the grapevine cultivar. As shown in Fig. 1a, *F. mediterranea* developed faster on Cabernet Sauvignon until nine dpi than on the other cultivars. *F. mediterranea* demonstrated the slowest growth on Ugni blanc sawdust (Fig. 1a).

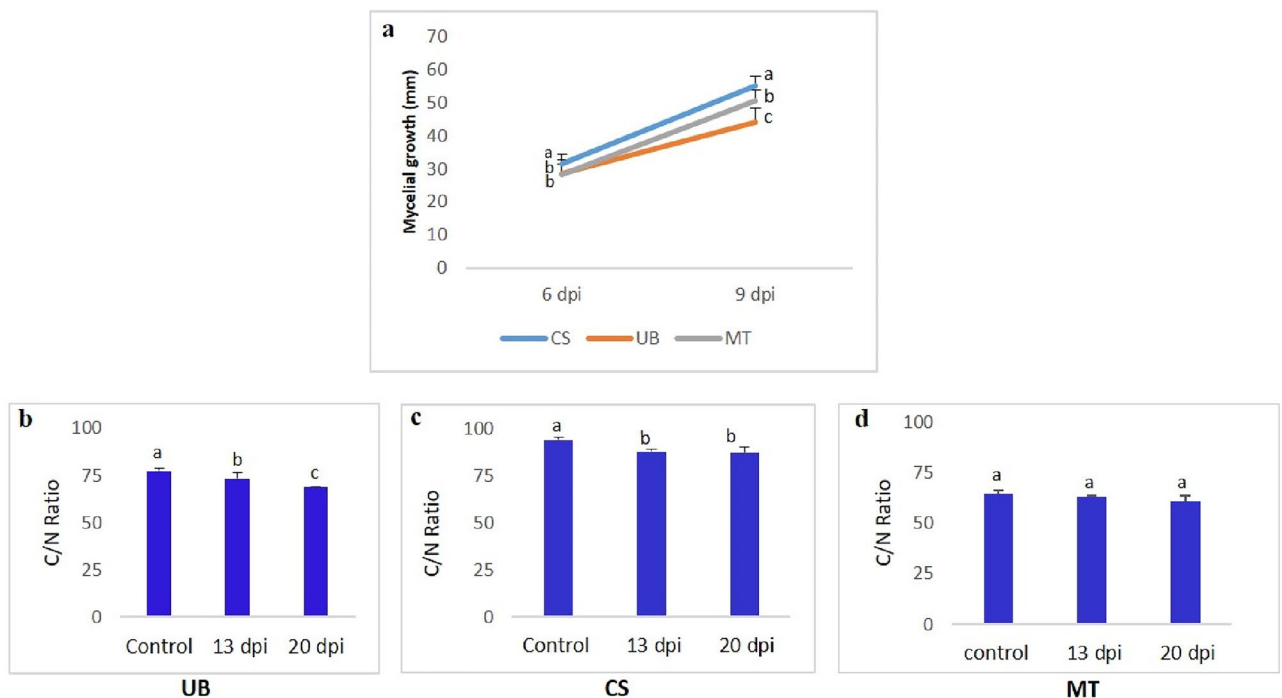


**Figure 1.** (a) Measurement of mycelial growth of *F. mediterranea* on sawdusts of tested cultivars (CS: Cabernet Sauvignon, UB: Ugni blanc, MT: Merlot) at 6 and 9 dpi. (b–d) Wood decay characterization after 13 and 20 days of the inoculation of *F. mediterranea* on sawdust of UB and CS. Different letters indicate significantly different at  $P \leq 0.05$ , according to the Newman and Keul's test after ANOVA. The error bar corresponds to the standard deviation of the mean.

### Degradation of wood of different grapevine cultivars by *F. mediterranea*

As shown in Fig. S1, the sawdust of all cultivars inoculated with *F. mediterranea* had a lighter color (more yellow) than the control sawdust at 13 and 20 dpi.

Carbon and nitrogen concentrations were measured in all cultivars after 13 and 20 days of incubation. A comparison of the C/N ratio at the three sampling times (T0 (control), T13, and T20) showed that the cultivar significantly affected ( $P=0.02$ ) wood degradation by *F. mediterranea*.

Contrary to the Merlot sawdust showing no difference in the C/N ratio at 13 and 20 dpi, the C/N ratios of Cabernet Sauvignon and Ugni blanc were significantly higher in sterile sawdust (control) than in other sawdust samples inoculated with *F. mediterranea* after 13 and 20 days of incubation (Fig. 1b–d). Interestingly, between 13 and 20 days of incubation, the C/N ratio significantly decreased in Ugni blanc sawdust, suggesting that *F. mediterranea* degrades the wood of this cultivar more efficiently (Fig. 1b). While the wood loss rates were 30 and 42% after 13 and 20 days, respectively, for Ugni blanc, the same rates were 15 and 19% for CS at 13 and 20 days, respectively.

To corroborate these results, we employed Magic-angle spinning (MAS) solid-state NMR to investigate wood degradation at the molecular level. MAS NMR is a powerful technique<sup>29–31</sup> for studying the molecular composition of wood, quantifying the structural polymeric components, and investigating wood degradation<sup>15</sup>. To measure the total wood decay, we performed <sup>13</sup>C-detected cross-polarization experiments on control wood samples of Cabernet Sauvignon and Ugni blanc. The resulting spectra showed similar <sup>13</sup>C spectral fingerprints composed of cellulose, hemicelluloses, and lignins (Fig. 2a). The peaks allow the identification of most chemical groups of these three polymers based on previously reported data<sup>32,33</sup>. By comparing the total peak intensity of the control samples with samples inoculated with *F. mediterranea*, we determined the total loss of wood (Fig. 2b), which was estimated to be ~10% for Cabernet Sauvignon and ~7% for Ugni blanc. Similar experiments using Merlot showed no detectable losses (data not shown). Thus, the NMR results were in line with the C/N ratio analysis, with *F. mediterranea* having a significant negative impact on Cabernet Sauvignon and Ugni blanc sawdust, whereas no noticeable effect was detected on Merlot sawdust.

### Degradation of Ugni blanc sawdust by *F. mediterranea*, *Paenibacillus* sp. (S231-2), and *P. amylolyticus* (S293) (applied individually or in combination)

As the wood degradation and the wood loss rates between 13 and 20 days of incubation with *F. mediterranea* was greater on Ugni blanc sawdust than with other cultivars, Ugni blanc was chosen to study the effects of the two selected bacterial strains on wood degradation.

#### *F. mediterranea*'s mycelial growth on grapevine wood sawdust

Mycelial growth of *F. mediterranea* was measured in all treatments inoculated with *F. mediterranea*. The results presented in Fig. 3a showed that *F. mediterranea*'s mycelial growth was more important in the presence of S231-2 and/or S293. Moreover, the co-inoculation of S293 with *F. mediterranea* strongly improved the mycelial growth of the pathogen.

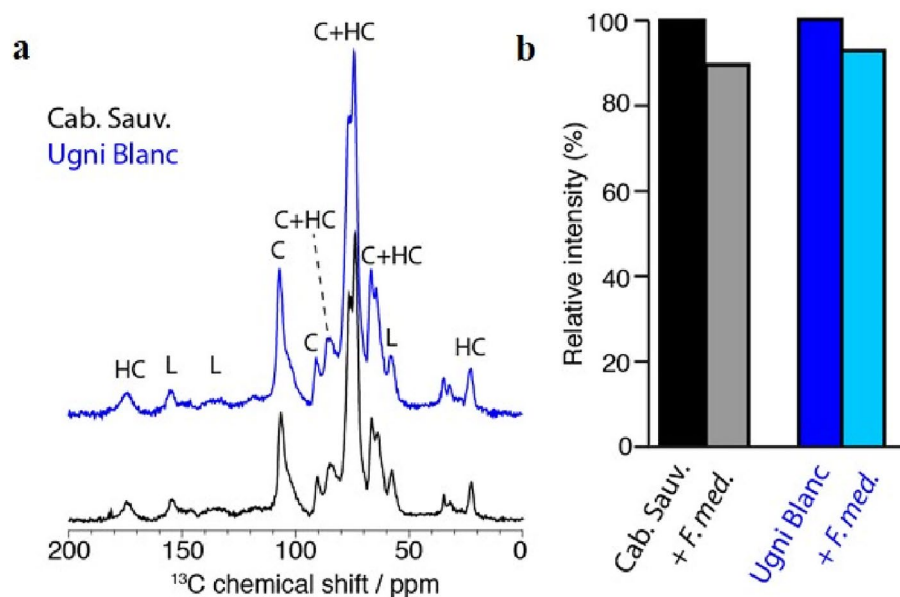


**Figure 2.** Solid-state NMR wood decay characterization after inoculation of *F. mediterranea* on Cabernet Sauvignon and Ugni blanc sawdusts. (a) <sup>13</sup>C cross-polarization spectra of CS and UB sawdust. (b) Total wood decay as measured by NMR intensity.

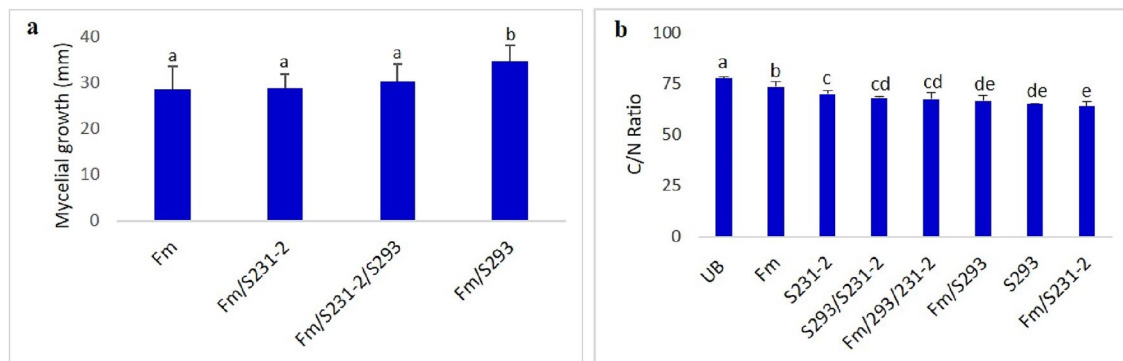


**Figure 3.** (a) Measurement of fungal mycelial growth on the sawdust of the different modalities inoculated with *F. mediterranea* (inoculated or not with bacterial strains). (b) C/N ratio at the end of the experimentation. UB: Ugni blanc, Fm: *F. mediterranea*, S231-2: *Paenibacillus* sp., S293: *P. amylolyticus*.

### Degradation of Ugni blanc sawdust inoculated with *F. mediterranea*, *Paenibacillus* sp. (S231-2), and *P. amylolyticus* (S293) (inoculated individually or in combination)

As presented in Figs. 3b, S2 degradation in all treatments (inoculated with *F. mediterranea*) was significantly higher than that in the control (not inoculated). Interestingly, the bacterial strains inoculated alone (individually or in combination) significantly degraded grapevine wood powder, indicating that the bacteria could degrade grapevine wood into small fine particles. Based on the C/N ratio, the bacterial strains applied individually coupled with *F. mediterranea* to grapevine wood sawdust resulted in greater degradation than those inoculated with both bacterial strains coupled with *F. mediterranea* (Fig. 3b). The highest wood degradation was observed in wood co-inoculated with *Paenibacillus* sp. (S231-2) and *F. mediterranea* (Fig. 3b). However, the results observed above showed that mycelial development of the pathogen in the presence of strain S231-2 was less important compared to other modalities inoculated with *P. amylolyticus* S293 and *F. mediterranea* or with both bacterial strains and *F. mediterranea*.

To analyze the effect of wood degradation more precisely, we complemented the quantitative C/N ratio analysis with an investigation using MAS NMR on the effect of *F. mediterranea* and bacterial strains S231-2 and S293, and their combination on Ugni blanc sawdust. Because the chemical shifts of cellulose, hemicellulose, and lignin can be identified in  $^{13}\text{C}$  CP experiments, the evolution of each biopolymer can be monitored under different inoculation conditions. Figure 4a shows various spectral regions of  $^{13}\text{C}$  CP experiments recorded on a control sample of Ugni blanc sawdust compared to sawdust inoculated with *F. mediterranea* and a combination of *Paenibacillus* sp. (S231-2) and *P. amylolyticus* (S293). The cellulose contribution was clearly observed at  $\sim 105$  ppm, which corresponded to the chemical shift of the  $\text{C}^{13}$  carbon (Fig. 4a). We observed comparable cellulose contributions among the three samples, as measured by the peak intensity, between the three samples. This indicates that wood degradation by *F. mediterranea* and the combination of S231-2 and 293 weakly affected cellulose. In contrast, two other major wood biopolymers, lignin and hemicellulose, showed noticeable changes between the three conditions. The contribution of lignin was observed in the spectral region of  $\sim 125$ – $155$  ppm, corresponding to  $^{13}\text{C}$  resonances of the aromatic groups of the guaiacyl, syringyl, and hydroxyphenyl units. A decrease in lignin contribution was detected, as indicated by a less intense signal (Fig. 4a). We estimated a decrease of  $\sim 35$ – $40\%$  in the lignin contribution (compared to cellulose) between the control sample and the sample inoculated with *F. mediterranea*. This observation is in line with the early NMR studies by Davis et al.<sup>34</sup>, who reported preferential lignin degradation by white-rot fungi<sup>34</sup>. Interestingly, a comparable decrease ( $\sim 35$ – $40\%$ ) was observed between the control and samples inoculated with strains S231-2 and S293, suggesting that these bacteria also have the ability to degrade lignin. The degradation of hemicellulose was investigated by monitoring the signal at  $\sim 20$  ppm, which corresponded to the methyl carbons of the acetyl groups. We detected a decrease in signal intensity of  $\sim 15$ – $20\%$  (compared to cellulose) between the control sample and the sample inoculated with *F. mediterranea* (Fig. 4a). The decrease was more significant for the samples inoculated with strains S231-2 and S293, with an estimated loss of intensity of  $\sim 20$ – $25\%$  (as compared to cellulose). In addition, we detected an increase in the signal in the spectral region of  $\sim 28$ – $35$  ppm (highlighted in yellow in Fig. 4a). Although precise chemical identification was not possible based on previous studies, we speculated that this signal contribution was related to the presence of  $\text{CH}_2$  groups that were not bound to oxygen<sup>34,35</sup>. This was likely due to the degradation products of hemicelluloses or products obtained after the reductive depolymerization of lignins. Overall, our results indicate a noticeable degradation of lignins and hemicelluloses after inoculation, which was more pronounced for lignins.

The synergistic effect of fungi and bacteria was investigated using MAS NMR experiments on Ugni blanc sawdust inoculated with a combination of *F. mediterranea* and bacterial strains S231-2 and S293. Following the same approach based on NMR signal comparison between the inoculated and control samples, we studied the degradation of the biopolymers. At the lignin level (Fig. 4b), a small decrease of  $\sim 5\%$  was detected, suggesting that the combination of *F. mediterranea* with strains S231-2 and 293 had a different degradation effect on sawdust than inoculation with the fungus or bacteria alone. The same observation was made for hemicelluloses with a signal decrease of  $\sim 10\%$  (Fig. 4b,c), while the signal pattern of cellulose was similar in the control and inoculated

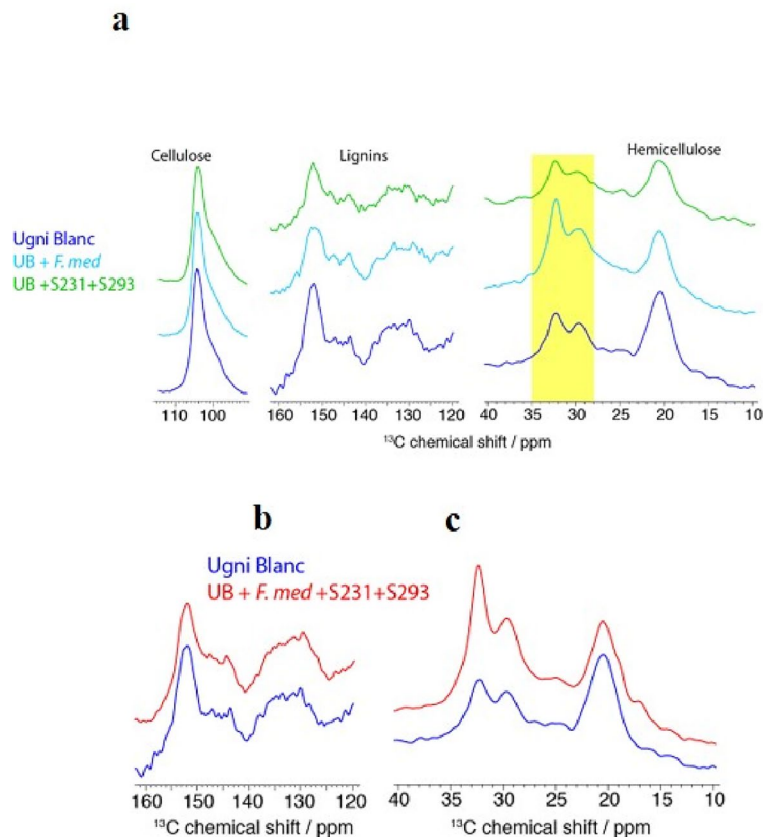


**Figure 4.** (a) Solid-state NMR wood decay characterization of Ugni blanc (UB) after inoculation of *F. mediterranea*, and *Paenibacillus* sp. (S231-2) and *P. amylolyticus* (S293).  $^{13}\text{C}$  CP spectra of UB (in blue) sawdust, inoculated with *F. mediterranea* (in cyan), and with a combination of S231-2 and S293 (in green). Spectral regions of cellulose, lignins and hemicelluloses are shown. The yellow rectangle corresponds to the chemical shift area of the degradation products. (b,c) Solid-state NMR wood decay characterization of Ugni blanc (UB) after inoculation of *F. mediterranea*, with *Paenibacillus* sp. (S231-2) and *P. amylolyticus* (S293).  $^{13}\text{C}$  CP spectra of Ugni blanc (UB) (in blue) sawdust and inoculated (in red). Spectral regions of lignins and hemicelluloses are shown.

samples (data not shown). The most important difference was observed in the spectral region of ~28–35 ppm, for which a drastic increase of ~50–60% (as compared to cellulose) was observed (Fig. 4b,c). Overall, the degradation effect of bacteria and fungi did not result from the simple addition of their degradation on each biopolymer, but this quantity of degradation products and depolymerized lignins greatly increased when fungal and bacterial communities were used in synergy.

### Genome analysis of S231-2 and S293

#### *Genomic features, taxonomic affiliation and COG categories*

The genomes of the strains S231-2 and S293 were sequenced, assembled, and annotated. Each genome had a total size of 7.39 Mb and 7.07 for S231-2 and S293, respectively, as well as an average G + C content of 45.7% and 45.8% and 6,715 and 6,244 coding genes, respectively (Fig. 5). The assessment of genome quality based on 468 markers showed a completeness of 99.85% for both strains with no contamination. The taxonomic placement based on Average Nucleotide Identity (ANI) provided a match with *P. amylolyticus* with a radius of 95.25%. The number of genes in each COG category did not change among the strains (Fig. 5a,b), as revealed by the Circos simulation (Fig. 5c). However, 28 genes associated with subsystems (Fig. 5d,e) in strain S231-2 were not predicted in strain S293, and 18 genes detected in S293 were not found in the genome of S231-2 (Tables S3, S4).

#### *Genes predicted to be involved in lignin, cellulose and hemicellulose degradation*

In addition to other clusters of ortholog groups, several genes involved in carbohydrate transport and metabolism were predicted using RAST or eggno3 annotation. Genes possibly involved in lignin degradation (related to lignin-degrading auxiliary enzymes and lignin-modifying enzymes) were detected in the S231-2 and S293 genomes (Tables 1, S1, S2, and S5-S6-S4). During the initial stages of lignin degradation, extracellular enzymes are responsible for lignin depolymerization. Lignin-modifying enzymes (LME) and lignin-degrading auxiliary (LDA) enzymes are the two main groups of lignin-degrading enzymes<sup>36</sup>. Multiple lignin modification- and

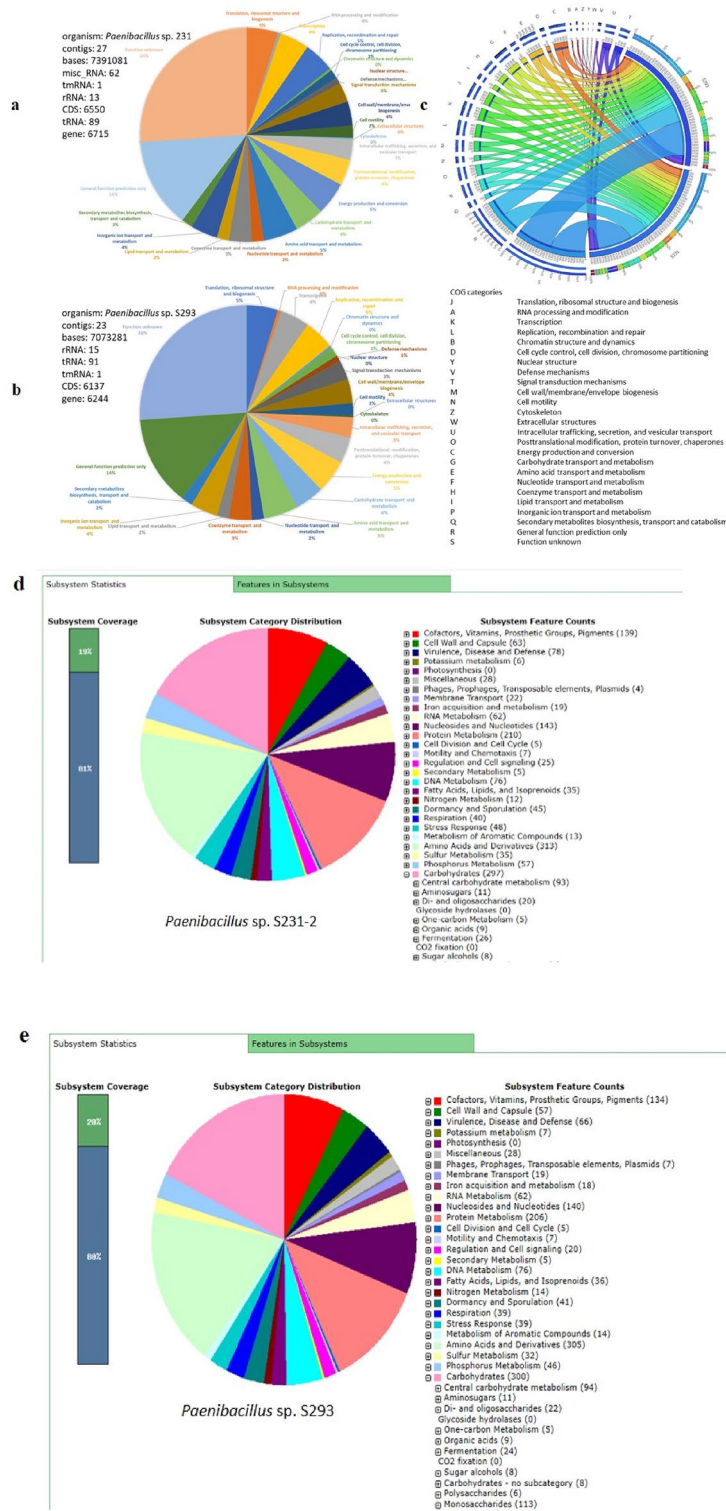


**Figure 5.** Genome annotation of S231-2 and S293 showing COG categories for each strain, a circos simulation to compare COG categories between strains as well as RAST annotation (enabling to see each subcategories including the numbers of genes related to xylose/xyloside degradation).

depolymerization-related genes were screened in the two genomes, including genes encoding LME, that is, small laccase-like multicopper oxidase genes, other laccases, dye-decolorizing peroxidase genes, manganese peroxidase-encoding genes, versatile peroxidases, and genes encoding LDA, such as glyoxal oxidases, aryl alcohol

|   | Number of genes |            |                          |
|---|-----------------|------------|--------------------------|
|   | S231-2          | S293       | S231-2/S293 <sup>a</sup> |
| Lignin-modifying enzymes                |                 |            |                          |
| Small laccase-like multicopper oxidases | 3               | 2          |                          |
| 1                                       | S231-2_06045    | –          | –                        |
| 2                                       | S231-2_02561    | S293_02831 | 97%                      |
| 3                                       | S231-2_03245    | S293_02343 | 97%                      |
| Other laccases                          | –               | –          |                          |
| Dye-decolorizing peroxidases            | –               | –          |                          |
| Manganese peroxidases                   | –               | –          |                          |
| Versatile peroxidases                   | –               | –          |                          |
| Lignin-degrading auxiliary activities   |                 |            |                          |
| Glyoxal oxidases                        | 14              | 15         |                          |
| Aryl alcohol oxidases                   | 1               | 1          |                          |
| Heme-thiolate haloperoxidases           | –               | –          |                          |
| Glucose dehydrogenases                  | 2               | 1          |                          |
| Pyranose 2-oxidases                     | –               | –          |                          |
| Cellobiose dehydrogenases               | –               | –          |                          |
| Cytochrome P450                         | 8               | 7          |                          |

**Table 1.** Number of genes of strains S231-2 and S298 putatively involved in lignin degradation, after analysis using eggNOG annotation and functionally annotated genes. <sup>a</sup>Identities on protein level of *Paenibacillus* sp. S231-2 compared to S293.

oxidases, glucose dehydrogenases, pyranose 2-oxidases, cellobiose dehydrogenases, and cytochrome P450. Using eggNOG annotation and for strain 293: 2 multicopper oxidases, 15 glyoxal oxidases, 1 aryl alcohol oxidase, 1 glucose dehydrogenase, and 7 cytochrome P450 related genes were detected. In strain S231-2, 3 multicopper oxidases, 14 glyoxal oxidases, 1 aryl alcohol oxidase, 2 glucose dehydrogenases, and 8 cytochrome P450 related genes were detected (Tables 1 and S5–S6).

Furthermore, we analyzed all gene clusters related to carbohydrate-active enzymes (CAZy) to gain a better understanding of the functions of carbohydrate-related genes encoding auxiliary activities, carbohydrate-binding modules, carbohydrate esterases, glycoside hydrolases, glycosyltransferases, and polysaccharide lyases (Fig. 6). In the CAZyme database, lignin-degrading enzymes are subdivided into the AA class, which are redox enzymes that act in conjunction with CAZymes. Lignin-oxidizing enzymes (LO) are in the AA1, AA2, and AA3 classes, and lignin-degrading auxiliary enzymes (LD) in the AA4, AA5, AA6, and AA8 classes. Genome analysis using the CAZyme database predicted that strains S231-2 and S293 had only one AA-related gene (AA7) that was not associated with lignin degradation. Using CAZyme annotation, we could not detect any genes related to lignin degradation. However, it is known that bacterial genes involved in lignin degradation are not included in the CAZyme database, except if their products carry a carbohydrate-binding module (CBM)<sup>37</sup>.

Genome analyses of strains S231-2 and S293 predicted several genes in each strain related to glycosyl hydrolase (GH) families, as well as subfamilies, such as GH1, GH105, GH18, GH2, GH3, and GH32 (with all having several different activities), GH38 (mannosidase, EC 3.2.1.-), GH42 ( $\beta$ -galactosidase, EC 3.2.1.23 or  $\alpha$ -L-arabinopyranosidase, EC 3.2.1.-), GH43\_24 (exo- $\beta$ -1,3-galactanase, and EC 3.2.1.145) containing at least five sequences for each strain (Fig. 6). All of these glycosyl hydrolases are involved in the degradation of hemicellulose (with glucosidase, xylosidase, mannosidase, galactase, rhamnase, and arabinase) or in cellulose degradation (such as GH1 and GH3). Other genes related to the CBM, PL (Polysaccharide lyases), CE (Carbohydrate esterases) and GT (Glycosyltransferases) were detected in each genome (Fig. 6). Six genes involved in xylose (xyloside) degradation were further predicted in each genome, with *XylA* coding for a xylose isomerase that catalyzes the conversion of D-xylose to D-xylulose, *XylB* coding for a xylulose kinase that catalyzes the phosphorylation of D-xylulose to D-xylulose 5-phosphate, *XynT* coding for a xyloside transporter, and xylosidase for both strains (Tables S1–S2).

### Genes predicted to be involved in plant–microbe and fungi–bacteria interaction

Using RAST and eggNOG annotation, analysis of the two bacterial genomes enabled the detection of protein-encoding genes that were predicted to be involved in plant–microbe and microbe–microbe interactions, including motility and chemotaxis, biofilm formation, sugar and nutrient metabolism, siderophore and iron transport, auxin synthesis, nitrogen metabolism, as well as genes related to osmotic stress, oxidative stress, detoxification, and several other genes (Tables S1–S4). Interestingly, the strains S231-2 and S293 possessed several genes that can contribute to arsenic resistance. Several gene clusters involved in the metabolism of vitamins, such as biotin (B7), thiamine (B1), pyridoxine (B6), cobalamine (B12), and phyloquinone (K2), were also detected during the analyses of the genomes of strains S231-2 and S293, but with a higher number of predicted genes for S293 (Tables S1–S2 and S5–S6). According to previous studies, some of these genes, such as those involved in vitamin B production, may also be involved in fungal growth stimulation<sup>38,39</sup>.

|     | S231-2     | S293 |     | S231-2    | S293                     |    | S231-2      | S293        |    | S231-2 | S293        |           |   |   |
|-----|------------|------|-----|-----------|--------------------------|----|-------------|-------------|----|--------|-------------|-----------|---|---|
| AA  | 1          | 1    |     | 1         | 1                        | GH | GH1.hmm     | 16          | 14 | GH     | GH31.hmm    | 1         | 1 |   |
| CBM | 65         | 63   | CBM | CBM12.hmm | 3                        | 1  | GH10.hmm    | 4           | 4  | GH     | GH32.hmm    | 5         | 6 |   |
| CE  | 39         | 40   |     | CBM20.hmm | 1                        | 1  | GH105.hmm   | 9           | 9  |        | GH35.hmm    | 3         | 3 |   |
| GH  | 214        | 209  |     | CBM22.hmm | 3                        | 3  | GH106.hmm   | 2           | 2  |        | GH36.hmm    | 1         | 2 |   |
| GT  | 44         | 44   |     | CBM3.hmm  | 6                        | 6  | GH109.hmm   | 8           | 8  |        | GH38.hmm    | 5         | 6 |   |
| PL  | 15         | 15   |     | CBM32.hmm | 11                       | 11 | GH11.hmm    | 1           | 1  |        | GH39.hmm    | 1         | 1 |   |
|     |            |      |     | CBM34.hmm | 3                        | 3  | GH112.hmm   | 1           | 1  |        | GH4.hmm     | 4         | 3 |   |
|     |            |      |     | CBM35.hmm | 2                        | 5  | GH113.hmm   | 1           | 1  |        | GH42.hmm    | 6         | 5 |   |
| CE  | CE1.hmm    | 7    | 7   | CBM36.hmm | 3                        | 3  | GH120.hmm   | 0           | 1  |        | GH43_1.hmm  | 1         | 1 |   |
|     | CE12.hmm   | 4    | 4   | CBM4.hmm  | 4                        | 4  | GH125.hmm   | 3           | 3  |        | GH43_10.hmm | 2         | 2 |   |
|     | CE13.hmm   | 5    | 5   | CBM42.hmm | 2                        | 2  | GH126.hmm   | 1           | 1  |        | GH43_11.hmm | 2         | 1 |   |
|     | CE14.hmm   | 2    | 2   | CBM46.hmm | 3                        | 3  | GH127.hmm   | 1           | 2  |        | GH43_12.hmm | 4         | 4 |   |
|     | CE17.hmm   | 2    | 2   | CBM48.hmm | 1                        | 1  | GH129.hmm   | 1           | 1  |        | GH43_16.hmm | 2         | 2 |   |
|     | CE2.hmm    | 1    | 1   | CBM50.hmm | 1                        | 1  | GH13_14.hmm | 2           | 2  |        | GH43_22.hmm | 3         | 3 |   |
|     | CE3.hmm    | 1    | 1   | CBM54.hmm | 1                        | 1  | GH13_2.hmm  | 1           | 1  |        | GH43_23.hmm | 1         | 1 |   |
|     | CE4.hmm    | 14   | 14  | CBM6.hmm  | 4                        | 4  | GH13_20.hmm | 3           | 3  |        | GH43_24.hmm | 6         | 6 |   |
|     | CE8.hmm    | 2    | 2   | CBM61.hmm | 1                        | 0  | GH13_29.hmm | 1           | 1  |        | GH43_26.hmm | 2         | 2 |   |
|     | CE9.hmm    | 1    | 1   | CBM62.hmm | 1                        | 0  | GH13_31.hmm | 3           | 3  |        | GH43_34.hmm | 1         | 1 |   |
|     |            |      |     | CBM63.hmm | 1                        | 1  | GH13_5.hmm  | 1           | 1  |        | GH43_35.hmm | 0         | 1 |   |
| PL  | PL1.hmm    | 1    | 1   | CBM66.hmm | 4                        | 4  | GH13_9.hmm  | 1           | 1  |        | GH43_4.hmm  | 2         | 2 |   |
|     | PL1_2.hmm  | 1    | 1   | CBM67.hmm | 3                        | 2  | GH130.hmm   | 3           | 3  |        | GH43_5.hmm  | 1         | 1 |   |
|     | PL1_8.hmm  | 1    | 1   | CBM9.hmm  | 6                        | 6  | GH140.hmm   | 1           | 1  |        | GH48.hmm    | 1         | 1 |   |
|     |            |      |     |           |                          |    | GH146.hmm   | 1           | 1  |        | GH5.hmm     | 1         | 0 |   |
|     | PL10_1.hmm | 1    | 1   |           |                          |    | GH148.hmm   | 1           | 0  |        | GH5_35.hmm  | 2         | 3 |   |
|     | PL11.hmm   | 3    | 3   | GT        | GT1.hmm                  | 1  | 2           | GH151.hmm   | 2  | 2      |             | GH5_4.hmm | 2 | 2 |
|     |            |      |     |           | GT2_Glyco_transf_2_3.hmm | 4  | 4           | GH16_21.hmm | 1  | 1      |             | GH5_8.hmm | 1 | 1 |
|     | PL11_2.hmm | 1    | 1   |           | GT2_Glycos_transf_2.hmm  | 15 | 15          | GH16_3.hmm  | 2  | 2      |             | GH51.hmm  | 4 | 4 |
|     | PL12.hmm   | 1    | 1   |           | GT26.hmm                 | 2  | 2           | GH18.hmm    | 6  | 6      |             | GH52.hmm  | 1 | 1 |
|     | PL29.hmm   | 1    | 1   |           | GT28.hmm                 | 3  | 3           | GH2.hmm     | 8  | 8      |             | GH53.hmm  | 4 | 3 |
|     | PL3_1.hmm  | 1    | 1   |           |                          |    | GH23.hmm    | 3           | 2  |        | GH6.hmm     | 1         | 1 |   |
|     |            |      |     |           | GT35.hmm                 | 1  | 1           | GH25.hmm    | 1  | 1      |             | GH67.hmm  | 1 | 1 |
|     | PL33_2.hmm | 1    | 1   |           | GT4.hmm                  | 9  | 9           | GH26.hmm    | 2  | 2      |             | GH68.hmm  | 0 | 1 |
|     | PL4_1.hmm  | 1    | 1   |           | GT5.hmm                  | 1  | 1           | GH27.hmm    | 2  | 2      |             | GH74.hmm  | 2 | 2 |
|     | PL9_1.hmm  | 1    | 1   |           | GT51.hmm                 | 4  | 4           | GH28.hmm    | 2  | 1      |             | GH78.hmm  | 4 | 3 |
|     | PL9_2.hmm  | 1    | 1   |           | GT83.hmm                 | 1  | 1           | GH29.hmm    | 4  | 4      |             | GH8.hmm   | 1 | 1 |
|     |            |      |     |           | GT84.hmm                 | 1  | 1           | GH3.hmm     | 20 | 18     |             | GH81.hmm  | 1 | 1 |
|     |            |      |     |           | GT94.hmm                 | 1  | 1           | GH30_2.hmm  | 1  | 1      |             | GH85.hmm  | 1 | 1 |
|     |            |      |     |           |                          |    | GH30_3.hmm  | 2           | 2  |        | GH88.hmm    | 3         | 2 |   |
|     |            |      |     |           |                          |    | GH30_5.hmm  | 2           | 2  |        | GH9.hmm     | 1         | 1 |   |
|     |            |      |     |           |                          |    | GH30_8.hmm  | 1           | 1  |        | GH94.hmm    | 2         | 2 |   |
|     |            |      |     |           |                          |    |             |             |    |        | GH95.hmm    | 3         | 4 |   |

**Figure 6.** Carbohydrate-active enzymes (CAZymes) related genes of strain S231-2 and S293 assessed with dbCAN2. CBM: carbohydrate-binding modules, CE: Carbohydrate esterases, GT: Glycosyltransferases, PL: Polysaccharide lyases, AA: Auxiliary activities.

### Biosynthetic gene clusters involved in secondary metabolite production

A total of 17 and 16 gene clusters likely involved in secondary metabolite production were identified in strains S231-2 and S293, respectively, using AntiSmash 7.0<sup>40</sup>. The core biosynthetic genes in the 16 common clusters were 94% or more identical at the protein level, indicating homologous biosynthesis clusters in the strains S231-2 and S293 (Table 2). Of these, one non-ribosomal peptide synthetase (NRPS) cluster encodes a polymyxin type, as indicated by >90% identity at the protein level of the biosynthesis genes compared to the verified polymyxin producer *P. alvei*<sup>41</sup>. One NRPS polyketide synthase (PKS)- hybrid cluster has 50–60% identity at the protein level to paenilarvin of *P. larvae*<sup>42</sup> in three genes, but the fourth is missing in strains S231-2 and S293 (Table 2). Therefore, a metabolite with similarities to paenilarvin is possible in S231-2 and S293, but the exact structure is certainly different. The complete gene cluster encoding for the siderophore bacillopaline from *P. mucilaginosus*<sup>43</sup> is more than 60% identical, on protein level, in both strains S231-2 and S293. The production of bacillopaline, a closely related siderophore, is likely to occur in both strains.

The identities of the potentially produced metabolites in the remaining secondary metabolite clusters are unknown. These additional metabolites include two NRPS, three PKS-NRPS hybrids, two type 1 PKS, one siderophore, one terpenoid (potentially involved in carotenoid production), and four ribosomally synthesized and post-translationally modified peptides (RiPPs). Strain S231-2 contains additionally a cyclic lactone auto-inducer peptide (Table 2). Raw sequence data for the bacterial genomes of strains S231-2 and S293 have been deposited in the National Center for Biotechnology Information (NCBI). They can be accessed under the name BioProject ID PRJNA1015190.

### Discussion

Fungi have historically been considered as the dominant pathogens involved in wood decay because of their ability to degrade lignocellulosic biopolymers<sup>44,45</sup>. The role of Ascomycota in grapevine wood disease has been extensively studied, but there is a lack of information regarding Basidiomycota members, especially regarding their relationship with other microorganisms, such as bacteria. The mode of action of the basidiomycete, *F. mediterranea*, which is responsible for the development of white-rot, a key necrotic factor involved in Esca disease, has been recently reviewed<sup>10</sup>. The non-enzymatic process for destroying wood components is still being investigated<sup>10</sup>, and at the same time the synergistic relationship of bacteria with this fungus has also been initiated<sup>15</sup>.

In this study, we examined the susceptibility of three grapevine cultivars to *F. mediterranea*. Our results obtained with a microcosm system are in agreement with data in the literature reporting that the cultivar Ugni blanc is more susceptible to Esca disease than Cabernet Sauvignon and Merlot<sup>46,47</sup>. The NMR data suggest that *F. mediterranea* degrades lignins and hemicelluloses more intensely than cellulose. Basidiomycetes have sophisticated processes to selectively degrade lignin species<sup>48,49</sup> and here, we report a notable loss of lignin after



| Compound  | Query proteins <sup>a</sup>   | S231-2   |          |            | S293   |          |          | S231-2/S293 <sup>b</sup> |
|---|-------------------------------|--|----------|------------|--|----------|----------|--------------------------|
|   |                               | Protein ID   | Coverage | Identity   | Protein ID                                     | Coverage | Identity |                          |
| (1) NRP: Polymyxin/Colistin ( <i>P. alvei</i> )               | LR_PmxE                       | S231-2_05531   | 100%     | 92%        | S293_05341                                     | 100%     | 92%      | 99%                      |
|   | LR_PmxD                       | S231-2_05530   | 100%     | 97%        | S293_05342                                     | 100%     | 97%      | 99%                      |
|   | LR_PmxC                       | S231-2_05529   | 100%     | 95%        | S293_05343                                     | 100%     | 94%      | 97%                      |
|   | LR_PmxA                       | S231-2_05527   | 100%     | 91%        | S293_05345                                     | 100%     | 91%      | 98%                      |
|   | LR_PmxB                       | S231-2_05528   | 100%     | 91%        | S293_05344                                     | 100%     | 91%      | 98%                      |
| (2) NRP: Paenillarvin ( <i>P. larvae</i> ssp. <i>larvae</i> ) | AHD05677_NRPS                 | S231-2_03165   | 90.90%   | 49%        | S293_02262                                     | 90.90%   | 49%      | 98%                      |
|   | AHD05678_NRPS                 | S231-2_03165   | 61.10%   | 51%        | S293_02262                                     | 61.10%   | 51%      | 98%                      |
|   | AHD05679_NRPSPKS              | S231-2_03166   | 100%     | 55%        | S293_02263                                     | 100%     | 55%      | 98%                      |
|   | AHD05680_malonyl-transacylase | S231-2_03167   | 97.70%   | 60%        | S293_02264                                     | 97.70%   | 60%      | 99%                      |
| (3) Siderophore: Bacillopaline ( <i>P. mucilaginosus</i> )    | KNP414_01893_HP               | S231-2_04961   | 99.30%   | 62%        | S293_04966                                     | 99.30%   | 62%      | 100%                     |
|   | KNP414_01894_HP               | S231-2_04962   | 93.80%   | 60%        | S293_04965                                     | 93.80%   | 60%      | 100%                     |
|   | KNP414_01895_HP               | S231-2_04963   | 96.60%   | 66%        | S293_04964                                     | 96.60%   | 67%      | 98%                      |
|   | KNP414_01896_ABC              | S231-2_04964   | 100%     | 72%        | S293_04963                                     | 98.90%   | 73%      | 97%                      |
|   | KNP414_01897_ABC              | S231-2_04965   | 99.70%   | 73%        | S293_04962                                     | 99.70%   | 72%      | 99%                      |
|   | KNP414_01898_ABC              | S231-2_04966   | 93.90%   | 72%        | S293_04961                                     | 93.90%   | 72%      | 99%                      |
|   | KNP414_01899_ABC              | S231-2_04967   | 97.70%   | 70%        | S293_04960                                     | 97.70%   | 70%      | 99%                      |
|   | KNP414_01900_ABC              | S231-2_04968   | 100%     | 64%        | S293_04959                                     | 100%     | 64%      | 97%                      |
| KNP414_01901_HP   | S231-2_04969                  | 97.80%   | 69%      | S293_04958 | 100%   | 67%      | 99%      |                          |
| Other AntiSmash 7.0 predictions:                              |                               | Region in S231-2 <sup>c</sup>                          |          |            | Region in S293                                 |          |          |                          |
| (4) NRPS <sup>d</sup>   |                               | S231-2_01215   |          |            | S293_00659                                     |          |          | 99%                      |
| (5) NRPS  |                               | S231-2_04511   |          |            | S293_03180                                     |          |          | 99%                      |
| (6) NRPS-PKS <sup>e</sup> hybrid                              |                               | S231-2_02719, S231-2_02720                             |          |            | S293_02986, S293_02987                         |          |          | 98–99%                   |
| (7) NRPS-PKS hybrid   |                               | S231-2_04595, S231-2_04593, S231-2_04592, S231-2_04589 |          |            | S293_03268, S293_03266, S293_03265, S293_03262 |          |          | 99%                      |
|   |                               | S231-2_06456, S231-2_06457, S231-2_06458, S231-2_06459 |          |            | S293_06028, S293_06029, S293_06030, S293_06031 |          |          |                          |
| (8) NRPS-PKS hybrid   |                               | S231-2_00526   |          |            | S293_01351                                     |          |          | 99–100%                  |
|   |                               | S231-2_00790   |          |            | S293_01088                                     |          |          |                          |
| (9) Type 3 PKS  |                               | S231-2_01510   |          |            | S293_00361                                     |          |          | 99%                      |
| (10) Type 3 PKS   |                               | S231-2_04083   |          |            | S293_04410                                     |          |          | 100%                     |
| (11) RiPP <sup>f</sup> : Lassopeptide                         |                               | S231-2_05316   |          |            | S293_04789                                     |          |          | 100%                     |
| (12) RiPP: Proteusin  |                               | S231-2_05427   |          |            | S293_04680                                     |          |          | 100%                     |
| (13) RiPP: lanthipeptide                                      |                               | S231-2_02093   |          |            | n.d  |          |          | 99%                      |
| (14) RiPP: lanthipeptide                                      |                               | S231-2_04289; S231_04292; S231-2_04293                 |          |            | S293_04215, S293_04212, S293_04211             |          |          | 98%                      |
| (15) Cyclic-lactone-autoinducer                               |                               | S231-2_03531   |          |            | S293_03993                                     |          |          | –                        |
| (16) Siderophore: IucA/IucC-like                              |                               |  |          |            |  |          |          | 94–100%                  |
| (17) Terpene  |                               |  |          |            |  |          |          | 98%                      |

**Table 2.** Predicted secondary metabolites in *Paenibacillus* sp. S231-2 and S293. Capacity of the production of NRPs, polymyxin and a paenillarvin-like compound and the siderophore bacillopaline as well as predicted secondary metabolites by antiSMASH 7.0. <sup>a</sup>Identities and coverage of complete cluster predicted by AntiSmash 7.0 are shown as identities in comparison to the known producers *P. alvei* LR, *P. larvae* ssp. *larvae* DSM 25,430 and *P. mucilaginosus* KNP414. <sup>b</sup>Identities on protein level of *Paenibacillus* sp. S231-2 compared to S293. <sup>c</sup>Core synthesis proteins of the potential secondary metabolite clusters. <sup>d</sup>NRPS: non-ribosomal peptide synthetase. <sup>e</sup>PKS: polyketide synthase. <sup>f</sup>RiPP: ribosomally synthesized and post-translationally modified peptides.

inoculation with *F. mediterranea*. Overall, we can hypothesize that in the vineyards, the difference in Esca-susceptibility between the tested cultivars could be explained, at least partly, by the different levels of wood degradation caused by *F. mediterranea* activity.

The roles of bacteria and their association with *F. mediterranea* in the degradation of grapevine wood were investigated. Because of the presence of numerous bacteria in all grapevine wood tissues, that are, healthy and necrotic<sup>50</sup>, their role in Esca needs to be investigated to better understand this Esca pathosystem. Because we showed that Ugni blanc was the most susceptible cultivar, its sawdust was used as a model to study the role of cellulolytic and xylanolytic bacterial strains in wood degradation. To the best of our knowledge, we showed for the first time that two bacterial strains of the genus *Paenibacillus* (S231-2 and S293) could increase the degradation of Ugni blanc wood colonized by *F. mediterranea*. Both strains were isolated from cordon wood tissues of Sauvignon blanc cultivar<sup>15</sup>. The highest wood degradation was obtained with the association of *F. mediterranea* with the bacterial strain S231-2 (*Paenibacillus* sp.). A similar increase in Cabernet Sauvignon sawdust degradation

was obtained by the co-inoculation of another strain of *Paenibacillus* (S150) with *F. mediterranea*. These results confirm those obtained with other bacteria that enhance the degradation of wood from other plants by wood-rotting basidiomycetes, such as *Trametes versicolor* and *Phanerochaete chrysosporium*<sup>21–24</sup>. For example, the co-culture of the fungus *T. versicolor* with *Cupriavidus* sp. TN6W-26 and *Enterobacter* sp. TN6W-26 enhanced the lignin degradation activity of this fungus<sup>21</sup>.

NMR data indicated a slight preference for hemicellulose degradation when comparing bacterial and fungal inoculations. We speculate that because of the presence of shorter chains and exposed sugar moieties, hemicelluloses are relatively easy to degrade, and our results suggest that bacterial strains S231-2 and S293 are more prone to degrade them.

Hoppe et al.<sup>51</sup> reported that the degradation of wood polymer structures increased the wood moisture content and the access of microorganisms to the wood. As bacteria have been reported to benefit from high wood moisture, thereby contributing to its decomposition<sup>52</sup>, the ability of bacterial strains S231-2 and/or S293 to degrade Ugni blanc grapevine wood on their own could also be explained by the increasing water availability in the degraded wood. Moreover, numerous genes which encode for enzymes involved in xylose (xyloside), cellulose, hemicellulose, and lignin degradation and modification were detected in the genomes of strains S231-2 and S293.

Although the greatest degradation was observed when S231-2 (*Paenibacillus* sp.) was co-inoculated with *F. mediterranea* on Ugni blanc sawdust, this was not associated with an increased growth of *F. mediterranea* mycelia, unlike the increased mycelial growth observed in the presence of strain S293. We hypothesized that the bacterial strains interacted differently with *F. mediterranea* during wood degradation processes; S231-2 may predispose sawdust to fungal attacks, and S293 (*P. amylolyticus*) may directly improve fungal growth. Among the possible modes-of-action of bacteria, it has been reported that bacteria can stimulate the fungal wood degradation by producing fungal growth-promoting substances, especially vitamins, and/or by stimulating certain enzymatic activities through the production of degradation effectors<sup>53,54</sup>. Our results are consistent with this, as we found genes which encode products related to vitamin metabolism in the genome of each strain.

In addition, the complete genome provided further evidence for bacterial strains abilities to degrade wood components. In the two genome sequences, numerous genes encode enzymes potentially involved in the degradation of cellulose, hemicellulose and lignin. For instance, the presence of genes related to lignin-degrading auxiliary enzymes and lignin-modifying enzymes, which are possibly involved in lignin degradation, are correlated with the results obtained in the genomes of other lignin degrading bacteria, such as some strains of *Bacillus subtilis*, *Erwinia billingiae* and *Klebsiella variicola*<sup>55–57</sup>.

Both strains encode also secondary metabolites such as siderophores and NRPS polymyxin. These compounds specifically act against a group of microorganisms, especially gram-negative bacteria<sup>58</sup>, and the secondary metabolite and siderophore potential may be involved in shaping the community in Esca-infected tissues.

In wood microcosms, white-rot fungi have been reported to induce significant changes in the bacterial community composition<sup>23,59</sup>, and promote the growth of cellulolytic and xylanolytic bacterial strains with less inhibitory effects against these fungi<sup>22</sup>. In line with these observations, our NMR data suggest that the synergistic effect of *F. mediterranea* with strains S231-2 and S293 is not just a simple addition of their degradation ability, but that the increase in degradation products is higher when bacteria and fungi are inoculated together on Ugni blanc. In addition, NMR data showed that the signal intensities differed between sawdust inoculated with bacteria or *F. mediterranea*. A higher contribution was observed for the sample inoculated with this fungus, suggesting different degradation mechanisms for the two samples. This is consistent with known degradation mechanisms that differ between fungi and bacteria, due to the ability of the former to produce more wood-degrading enzymes<sup>36,49</sup>. Overall, our results indicate a notable degradation of lignins and hemicelluloses after inoculation, which was more pronounced for lignins.

The increase in Ugni blanc sawdust degradation compared to Cabernet Sauvignon and Merlot sawdust was not correlated with sawdust/wood colonization by *F. mediterranea*. Slower colonization associated with more efficient and faster wood degradation could explain this result.

All the results obtained with the three bacterial strains, S150<sup>15</sup>, S231-2, and S293, confirmed our hypothesis that some bacteria colonizing grapevines enhance the ability of fungi to degrade wood structures. It was also shown that these three bacterial strains, which directly degrade wood components, share a common feature: they belong to the *Paenibacillus* genus. Various species of *Paenibacillus* are able to produce glucanases, cellulases, chitinases, xylanases, and proteases that are implicated in the destruction of eukaryotic cell walls<sup>60–62</sup>. Recently, Tahir et al.<sup>63</sup> identified three strains of *Paenibacillus* sp. that degrade lignin, and they showed that *Paenibacillus* enzymes degrade and/or modify this wood biopolymer.

The results obtained in this study contribute to the current evidence that bacteria interact with fungi during wood decay<sup>16,64</sup>. For example, laccase-like multicopper oxidases have recently been associated with lignin degradation in several Gram-positive bacteria<sup>65</sup>, and similar genes, such as those related to small laccase-like multicopper oxidases, have been identified in the *Paenibacillus* strains S231-2 and S293, supporting their potential function in lignin degradation or modification, although the specific function of these proteins requires further characterization.

In conclusion, our results show that two *Paenibacillus* strains are involved alone in the degradation of grapevine wood, but their association with the fungus, *F. mediterranea*, increased this wood degradation. *F. mediterranea* and bacterial degradation pathways of different grapevine cultivars will provide answers to understand the role of microbial communities in Esca and GTDs pathosystems, and to propose more efficient control management. To determine the frequency of these microbial interactions in the wood of mature grapevines would also be relevant in the future.

## Methods

### Microorganisms and culture conditions

#### *Selected bacteria and bacterial inoculum*

The two bacterial strains used were selected from a previous experiment on wood microcosms (i.e., the medium was made of sawdust grapevine), as they displayed strong cellulase and xylanase activities and did not inhibit the growth of *F. mediterranea* mycelia<sup>15</sup>.

For inoculations, the bacterial suspensions of strain S231-2 (*Paenibacillus* sp.) and S293 (*P. amylolyticus*) were prepared as follows: Liquid cultures were obtained by inoculating Erlenmeyer flasks containing TSB with bacterial colonies pre-grown on TSA and then by incubating them at 28 °C for 24 h using an orbital shaker at 150 rpm. Liquid cultures were then centrifuged twice at 5000 rpm for 10 min, and the pellets were resuspended in sterile water to obtain liquid suspensions for use in the microcosm experiments. The bacterial concentration of each suspension obtained was estimated at  $2 \times 10^8$  CFU mL<sup>-1</sup>.

#### *Fomitiporia mediterranea* strain and culture conditions

*F. mediterranea* strain (PHCO36) used in this study was obtained from the INRAE-UMR 1065 SAVE collection (Bordeaux, France). The fungus was stored at 4 °C on Malt Agar (MA) medium. The cells were subcultured on MA and incubated at 28 °C for 7 d before use in the microcosm experiments.

### Plant material

Grapevine cuttings of Cabernet Sauvignon, Merlot, and Ugni blanc cultivars, originating from INRAE experimental vineyards, were used for the microcosm experiments. Depending on the experiment, the wood of each cultivar was crushed and sieved (1-mm mesh to obtain sawdust) and then autoclaved (20 min, 120 °C) twice, for 2 days in between. Sawdust was plated on TSA and MA media to determine the initial sterility. After incubation at 28 °C for 7 days, no microbial growth was detected.

### Microcosm experimentations

#### *Susceptibility of three cultivars of grapevine to F. mediterranea*

**Experimental design.** Experiments were carried out with *F. mediterranea* in microcosms (90 mm Petri plates sealed with adhesive tape) containing 2 g of sawdust wood from each cultivar. A mycelial disk (5 mm in diameter) taken from the margin of a 7-day-old fungal colony was placed on sawdust and inoculated with 5 mL of sterile distilled water. Control plates were inoculated with 5 mL of sterile distilled water only. Each plate was sealed with transparent adhesive tape and incubated for 13 or 20 d at 28 °C in the dark. Two treatments, each applied to 35 microcosms, were tested as follows: (i) controls containing sawdust from each cultivar with sterile water, and (ii) experimental group containing sawdust from each cultivar with *F. mediterranea* and sterile water.

**Fungal growth measurement.** To evaluate any possible variations in the growth of *F. mediterranea* on the wood of the three cultivars, fungal growth was assessed by measuring mycelial growth in all replicates of each treatment (35 microcosms by cultivar) on days six and nine post inoculation.

**Estimation of the wood degradation.** After 13 days of incubation, the degradation of sawdust in four microcosms was assessed by measuring the C and N content in the wood by the Dumas method using a VarioMax cube elemental analyzer at the USRAVE precincts (USRAVE, INRAE Aquitaine, France). The C/N ratio provides information on changes in the chemical composition of organic matter. This ratio is an important variable correlated with organic matter mass loss, especially during the decomposition process<sup>22,23,66–69</sup>. The size and color of the sawdust were observed and compared with those of the corresponding control.

### Effect of *P. amylolyticus* (S293), *Paenibacillus* sp. (S231-2), and *F. mediterranea* co-culture on Ugni blanc wood degradation

#### *Experimental design*

Ugni blanc sawdust was used to study the effects of two bacterial strains, S231-2 (*Paenibacillus* sp.) and S293 (*P. amylolyticus*), on wood degradation, with or without *F. mediterranea*. The inoculation of *F. mediterranea* was done as previously described. For bacterial inoculation, 5 mL of the bacterial cell suspension was added to the microcosms inoculated with only one bacterial strain. In the microcosms inoculated with both bacterial strains, only 2.5 mL of each bacterial cell suspension was added. Each plate was sealed with transparent adhesive tape and incubated for 13 d at 28 °C in the dark.

Eight treatments, each applied on 25 microcosms, were tested (i) control containing Ugni blanc sawdust with sterile water; or Ugni blanc sawdust containing: (ii) *F. mediterranea* with sterile water; (iii) *F. mediterranea* and *P. amylolyticus* (S293) or *Paenibacillus* sp. (S231-2); (iv) *F. mediterranea*, *P. amylolyticus* (S293), and *Paenibacillus* sp. (S231-2); (v) *P. amylolyticus* (S293) or *Paenibacillus* sp. (S231-2); (vi) *P. amylolyticus* (S293) and *Paenibacillus* sp. (S231-2).

### Effects of *Paenibacillus* sp. (S231-2) and/or *P. amylolyticus* (S293) on the growth of *F. mediterranea*

To evaluate the effect of bacterial inoculation on the mycelial growth of *F. mediterranea* on the wood in the eight treatments described above, fungal growth was assessed by measuring the mycelial growth of all repetitions (25 microcosms) on day six post inoculation.

## Estimation of the wood degradation by measurement of C and N concentrations

Wood degradation was estimated by measuring the C and N concentrations in the sawdust of six microcosms after treatment at 13 dpi (day post inoculation) using the Dumas method with a VarioMax cube elemental analyzer at the USRAVE precincts (USRAVE, INRAE Aquitaine, France).

## Statistical analyses

The experimental data obtained from microcosm experimentations, were compared using analysis of variance (ANOVA), followed by the Newman–Keuls test ( $P=0.05$ ). These analyses were carried out with the STATBOX software (Version 6.6, grimmer Logiciels, Paris, <http://www.statbox.com>).

### *Estimation of the wood degradation by solid-state (NMR) spectroscopy*

MAS solid-state NMR spectroscopy experiments were performed on one microcosm a 7 T (300 MHz  $^1\text{H}$  Larmor frequency) Avance III spectrometer (Bruker Biospin) using a 4 mm dual CP-MAS DVT N-P/H probe. The MAS frequency was set to 11 kHz and the probe temperature was set to 6.85 °C. Proton decoupling (90 kHz, SPINAL-64) was applied during  $^{13}\text{C}$  direct acquisition. 1D  $^{13}\text{C}$  cross-polarization (CP) experiments (5120 scans) were performed using a contact time of 500  $\mu\text{s}$ .

## Genome contents of the bacterial strains *Paenibacillus* sp. (S231-2) and *P. amylolyticus* (S293)

The bacterial genomic DNA of each strain was extracted following a phenol–chloroform-based protocol after growing the strain in liquid TSB medium for 3 days and harvesting it by centrifugation at 6000 rpm for 3 min (as reported by Haidar et al<sup>15</sup> for strain S150). The bacterial pellets were resuspended in a lysis buffer (0.2 mg mL<sup>-1</sup> Proteinase K, 50 mM Tris–Cl, 1% SDS, 5 mM EDTA at pH 8 and 0.5 M NaCl) and incubated overnight (at 65 °C; 400 rpm). DNA from each strain was extracted twice using phenol–chloroform–isoamyl alcohol at a ratio of 25:24:1 and collected by centrifugation at 6,000 rpm for 3 min, as described previously<sup>38</sup>. Genomic DNA was purified using Amicon Ultra 0.5 mL 30 K Centrifugal Filter Units (Millipore, Cork, Ireland) and resuspended in sterile distilled water. Whole-genome shotgun sequencing of each strain was performed using an Illumina NovaSeq 6000 mode S2 (GATC Biotech, Konstanz, Germany), producing approximately 6.2 million paired-end reads of 150 bp. The Illumina reads were screened for the presence of PhiX using Bowtie 2 (v2.3.4.3)<sup>70</sup>; adapters were trimmed, and quality filtering was performed using FASTP (v0.19.5)<sup>71</sup>. The sequence length distribution and quality were checked using FastQC<sup>72</sup>. Genome assembly was performed with SPAdes v3.13.0<sup>72</sup>, and low-abundant (< 2 $\times$ ) and short (< 500 bp) contigs were discarded. The contigs were checked for the presence of contaminants using BlobTools v.1.1.1. The quality of genome assemblies was determined using QualiMap v2.2<sup>73</sup> and QUAST v5.0.0, and then genome completeness of the reconstructed genomes was evaluated using CheckM v1.2.2<sup>74</sup>. Gene annotation was carried out using Prokka v1.12<sup>75</sup> and the NCBI Prokaryotic Genome Annotation Pipeline (PGAP). Plasmid presence was determined using Mash v2.1 against the PLSDB database<sup>76</sup>. Putative plasmid contigs were screened for the presence of genes encoding the replication initiator protein, *repA*. For this purpose, a curated FASTA file with approximately 8,000 *repA* genes was generated from the plasmid genome sequences in NCBI. These *repA* sequences were used to build a database against which selected contigs were aligned using BLAST + v.2.10.0. These *repA* gene sequences were used to build a database against which the selected contigs were BLASTed. Functional annotation was performed using WebMGA for COG, the ClassicRAST (Rapid Annotation using Subsystem Technology) webserver (<http://rast.nmpdr.org>)<sup>77</sup> and the hierarchical orthology framework EggNOG 4.5<sup>78</sup>. The Carbohydrate-Active Enzyme (CAZy) families were ascertained using dbCAN2 based on the HMMER database. Proteins were annotated using the CAZy database<sup>79</sup>. Biosynthetic gene clusters and secondary metabolites were predicted using antiSMASH version 4.0.2<sup>80</sup>. To assign objective taxonomic classifications to the genome, the software toolkit GTDB-Tk v2.3.2 was used<sup>81,82</sup> using the Genome Taxonomy Database release version 214 (<https://gtdb.ecogenomic.org/>).

## Data availability

Raw sequence data for the bacterial genomes of strains S231-2 and S293 have been deposited in the National Center for Biotechnology Information (NCBI). They can be accessed under the name BioProject ID PRJNA1015190.

Received: 11 January 2024; Accepted: 2 July 2024

Published online: 09 July 2024

## References

- Gramaje, D., Úrbez-Torres, J. R. & Sosnowski, M. R. Managing grapevine trunk diseases with respect to etiology and epidemiology: Current strategies and future prospects. *Plant. Dis.* **102**, 12–39 (2018).
- Bertsch, C. et al. Grapevine trunk diseases: Complex and still poorly understood. *Plant. Pathol.* **62**, 243–265 (2013).
- Cragg, S. M. et al. Lignocellulose degradation mechanisms across the tree of life. *Curr. Opin. Chem. Biol.* **29**, 108–119 (2015).
- Hatakka, A. & Hammel, K. E. Fungal biodegradation of lignocelluloses. In *Industrial Applications* (ed. Hofrichter, M.) 319–340 (Springer, 2011).
- Purahong, W. et al. Are correlations between deadwood fungal community structure, wood physico-chemical properties and lignin-modifying enzymes stable across different geographical regions?. *Fungal. Ecol.* **22**, 98–105 (2016).
- Azevedo-Nogueira, F. The road to molecular identification and detection of fungal grapevine trunk diseases. *Front. Plant. Sci.* **13**, 960289 (2022).
- Fischer, M. A new wood-decaying basidiomycete species associated with esca of grapevine: *Fomitiporia mediterranea* (Hymenochaetales). *Mycol. Progress.* **1**, 315–324 (2002).
- Moretti, S. et al. *Fomitiporia mediterranea* M. Fisch., the historical Esca agent: A comprehensive review on the main grapevine wood rot agent in Europe. *Phytopathol. Mediterr.* **60**, 351–379 (2021).

9. Mugnai, L., Graniti, A. & Surico, G. Esca (Black Measles) and brown wood-streaking: Two old and elusive diseases of grapevines. *Plant. Dis.* **83**, 404–418 (1999).
10. Pacetti, A. *et al.* Grapevine wood-degrading activity of *Fomitiporia mediterranea* M. Fisch.: A Focus on the enzymatic pathway regulation. *Front. Microbiol.* **13**, 844264 (2022).
11. Awad, M., Giannopoulos, G., Mylona, P. V. & Polidoros, A. N. Comparative analysis of grapevine epiphytic microbiomes among different varieties, tissues, and developmental stages in the same terroir. *Appl. Sci.* **13**, 102 (2023).
12. Bruez, E. *et al.* Major changes in grapevine wood microbiota are associated with the onset of esca, a devastating trunk disease. *Environ. Microbiol.* **22**, 5189–5206 (2020).
13. Campisano, A. *et al.* Bacterial endophytic communities in the grapevine depend on pest management. *PLoS. ONE* **9**, e112763 (2014).
14. Zarraonaindia, I. *et al.* The soil microbiome influences grapevine-associated microbiota. *mBio* **6**, e02527–e2614 (2015).
15. Haidar, R. *et al.* Bacteria associated with wood tissues of Esca-diseased grapevines: Functional diversity and synergy with *Fomitiporia mediterranea* to degrade wood components. *Environ. Microbiol.* **23**, 6104–6121 (2021).
16. Wei, Y. *et al.* Improved lignocellulose-degrading performance during straw composting from diverse sources with actinomycetes inoculation by regulating the key enzyme activities. *Bioresour. Technol.* **271**, 66–74 (2019).
17. Kamimura, N., Sakamoto, S., Mitsuda, N., Masai, E. & Kajita, S. Advances in microbial lignin degradation and its applications. *Curr. Opin. Biotechnol.* **56**, 179–186 (2019).
18. Nargotra, P. *et al.* Microbial lignocellulolytic enzymes for the effective valorization of lignocellulosic biomass: A Review. *Catalysts.* **13**, 83 (2023).
19. Johnston, S. R., Boddy, L. & Weightman, A. J. Bacteria in decomposing wood and their interactions with wood-decay fungi. *FEMS Microbiol. Ecol.* **92**, fiw179 (2016).
20. Tláškal, V. & Baldrian, P. Deadwood-inhabiting bacteria show adaptations to changing carbon and nitrogen availability during decomposition. *Front. Microbiol.* **12**, 685303 (2021).
21. Valášková, V., de Boer, W., Klein Gunnewiek, P. J. A., Pospíšek, M. & Baldrian, P. Phylogenetic composition and properties of bacteria coexisting with the fungus *Hypholoma fasciculare* in decaying wood. *ISME. J.* **3**, 1218–1221 (2009).
22. Hervé, V., Ketter, E., Pierrat, J. C., Gelhaye, E. & Frey-Klett, P. Impact of *Phanerochaete chrysosporium* on the functional diversity of bacterial communities associated with decaying wood. *PLoS. ONE.* **11**, e0147100 (2016).
23. Hervé, V., Le Roux, X., Uroz, S., Gelhaye, E. & Frey-Klett, P. Diversity and structure of bacterial communities associated with *Phanerochaete chrysosporium* during wood decay: Bacteria of the white-rot mycosphere. *Environ. Microbiol.* **16**, 2238–2252 (2014).
24. Kamei, I. Co-culturing effects of coexisting bacteria on wood degradation by *Trametes versicolor*. *Curr. Microbiol.* **74**, 125–131 (2017).
25. Mesguida, O. *et al.* Microbial biological control of fungi associated with grapevine trunk diseases: A Review of strain diversity, modes of action, and advantages and limits of current strategies. *J. Fungi.* **9**, 638 (2023).
26. Mondello, V. *et al.* Grapevine trunk diseases: A review of fifteen years of trials for their control with chemicals and biocontrol agents. *Plant. Dis.* **102**, 1189–1217 (2018).
27. Haidar, R. *et al.* Synergistic effects of water deficit and wood-inhabiting bacteria on pathogenicity of the grapevine trunk pathogen *Neofusicoccum parvum*. *Phytopathol. Mediterr.* **59**, 473–484 (2020).
28. Haidar, R. *et al.* *Paenibacillus xylinteritus* sp. nov., a novel bacterial species isolated from grapevine wood. Preprint at <https://doi.org/10.1101/2022.12.09.519748> (2022).
29. Bardet, M., Foray, M. F. & Trân, Q.-K. High-resolution solid-state CPMAS NMR study of archaeological woods. *Anal. Chem.* **74**, 4386–4390 (2002).
30. Bardet, M. & Pournou, A. Fossil wood from the miocene and oligocene epoch: Chemistry and morphology. *Magn. Reson. Chem.* **53**, 9–14 (2015).
31. Mao, J., Holtman, K. M., Scott, J. T., Kadla, J. F. & Schmidt-Rohr, K. Differences between lignin in unprocessed wood, milled wood, mutant wood, and extracted lignin detected by <sup>13</sup>C Solid-State NMR. *J. Agric. Food. Chem.* **54**, 9677–9686 (2006).
32. Haw, J. F., Maciel, G. E. & Schroeder, H. A. Carbon-13 nuclear magnetic resonance spectrometric study of wood and wood pulping with cross polarization and magic-angle spinning. *Anal. Chem.* **56**, 1323–1329 (1984).
33. Kolodziejewski, W., Frye, J. S. & Maciel, G. E. Carbon-13 nuclear magnetic resonance spectrometry with cross polarization and magic-angle spinning for analysis of lodgepole pine wood. *Anal. Chem.* **54**, 1419–1424 (1982).
34. Davis, M. F., Schroeder, H. R. & Maciel, G. E. Solid-State <sup>13</sup>C nuclear magnetic resonance studies of wood decay. I. White rot decay of colorado blue spruce. *Holzforschung.* **48**, 99–105 (1994).
35. Koenig, A. B., Slighter, R. L., Salmon, E. & Hatcher, P. G. NMR Structural characterization of *Quercus alba* (White Oak) degraded by the brown rot fungus, *Laetiporus sulphureus*. *J. Wood. Chem. Technol.* **30**, 61–85 (2010).
36. Janusz, G. *et al.* Lignin degradation: Microorganisms, enzymes involved, genomes analysis and evolution. *FEMS Microbiol. Rev.* **41**, 941–962 (2017).
37. Drula, E. *et al.* The carbohydrate-active enzyme database: Functions and literature. *Nucleic. Acids. Res.* **50**, D571–D577 (2022).
38. del Barrio-Duque, A. *et al.* Beneficial endophytic bacteria-*Serendipita indica* interaction for crop enhancement and resistance to phytopathogens. *Front. Microbiol.* **10**, 2888 (2019).
39. del Barrio-Duque, A. *et al.* Interaction between endophytic Proteobacteria strains and *Serendipita indica* enhances biocontrol activity against fungal pathogens. *Plant. Soil.* **451**, 277–305 (2020).
40. Blin, K. *et al.* antiSMASH 7.0: New and improved predictions for detection, regulation, chemical structures and visualisation. *Nucleic. Acids. Res.* (2023).
41. Tambaou, F. *et al.* Characterization of the colistin (polymyxin E1 and E2) biosynthetic gene cluster. *Arch. Microbiol.* **197**, 521–532 (2015).
42. Sood, S. *et al.* Paenilarvins: Iturin family lipopeptides from the honey bee pathogen *Paenibacillus larvae*. *Chembiochem.* **15**, 1947–1955 (2014).
43. Morey, J. R. & Kehl-Fie, T. E. Bioinformatic mapping of opine-like zincophore biosynthesis in bacteria. *mSystems.* **5**, e00554–e620 (2020).
44. Dashtban, M., Schraft, H., Syed, T. A. & Qin, W. Fungal biodegradation and enzymatic modification of lignin. *Int. J. Biochem. Mol. Biol.* **1**, 36–50 (2010).
45. Goodell, B., Winandy, J. E. & Morrell, J. J. Fungal degradation of wood: Emerging data, new insights and changing perceptions. *Coatings.* **10**, 1210 (2020).
46. Bruez, E. *et al.* Overview of grapevine trunk diseases in France in the 2000s. *Phytopathol. Mediterr.* **52**, 262–275 (2013).
47. Cardot, C. *et al.* Comparison of the molecular responses of tolerant, susceptible and highly susceptible grapevine cultivars during interaction with the pathogenic fungus *Eutypa lata*. *Front. Plant. Sci.* **10**, 991 (2019).
48. Sánchez, C. Lignocellulosic residues: Biodegradation and bioconversion by fungi. *Biotechnol. Adv.* **27**, 185–194 (2009).
49. Zabel, R. A. & Morrell, J. J. Chapter Eight: Chemical changes in wood caused by decay fungi. In *Wood Microbiology* 2nd edn (eds Zabel, R. A. & Morrell, J. J.) 215–244 (Academic Press, 2020).
50. Bruez, E. *et al.* Bacteria in a wood fungal disease: Characterization of bacterial communities in wood tissues of esca-foliar symptomatic and asymptomatic grapevines. *Front. Microbiol.* **6**, 1137 (2015).

51. Hoppe, B. *et al.* A pyrosequencing insight into sprawling bacterial diversity and community dynamics in decaying deadwood logs of *Fagus sylvatica* and *Picea abies*. *Sci. Rep.* **5**, 9456 (2015).
52. Hu, Z. *et al.* Linking microbial community composition to C loss rates during wood decomposition. *Soil. Biol. Bioch.* **104**, 108–116 (2017).
53. Boer, W., Folman, L. B., Summerbell, R. C. & Boddy, L. Living in a fungal world: Impact of fungi on soil bacterial niche development. *FEMS Microbiol. Rev.* **29**, 795–811 (2005).
54. Murray, A. C. & Woodward, S. Temporal changes in functional diversity of culturable bacteria populations in Sitka spruce stumps. *Forest. Pathol.* **37**, 217–235 (2007).
55. dos Santos Melo-Nascimento, A. O. *et al.* Complete genome reveals genetic repertoire and potential metabolic strategies involved in lignin degradation by environmental ligninolytic *Klebsiella variicola* P1CD1. *PLoS. One* **15**, e0243739 (2020).
56. Qu, F., Cheng, H., Han, Z., Wei, Z. & Song, C. Identification of driving factors of lignocellulose degrading enzyme genes in different microbial communities during rice straw composting. *Bioresour. Technol.* **381**, 129109 (2023).
57. Zhao, S. *et al.* Lignin bioconversion based on genome mining for ligninolytic genes in *Erwinia billingiae* QL-Z3. *Biotechnol. Biofuels* **17**, 25 (2024).
58. Poirel, L., Jayol, A. & Nordmann, P. Polymyxins: Antibacterial activity, susceptibility testing, and resistance mechanisms encoded by plasmids or chromosomes. *Clin. Microbiol. Rev.* **30**, 557–596 (2017).
59. Folman, L. B., Klein Gunnewiek, P. J. A., Boddy, L. & de Boer, W. Impact of white-rot fungi on numbers and community composition of bacteria colonizing beech wood from forest soil. *FEMS Microbiol. Ecol.* **63**, 181–191 (2008).
60. Ghio, S. *et al.* Isolation of *Paenibacillus* sp. and *Variovorax* sp. strains from decaying woods and characterization of their potential for cellulose deconstruction. *Int. J. Biochem. Mol. Biol.* **3**, 352–364 (2012).
61. Grady, E. N., MacDonald, J., Liu, L., Richman, A. & Yuan, Z.-C. Current knowledge and perspectives of *Paenibacillus*: A review. *Microbiol. Cell. Fact.* **15**, 203 (2016).
62. Madhaiyan, M. *et al.* *Paenibacillus polysaccharolyticus* sp. Nov., a xylanolytic and cellulolytic bacteria isolated from leaves of Bamboo *Phyllostachys aureosulcata*. *Int. J. Syst. Evol. Microbiol.* **67**, 2127–2133 (2017).
63. Tahir, A. A. *et al.* Microbial diversity in decaying Oil Palm empty fruit bunches (OPEFB) and isolation of lignin-degrading bacteria from a tropical environment. *Microbes. Environ.* **4**, 161–168 (2019).
64. Johnston, S. R., Hiscox, J., Savoury, M., Boddy, L. & Weightman, A. J. Highly competitive fungi manipulate bacterial communities in decomposing beech wood (*Fagus sylvatica*). *FEMS Microbiol. Ecol.* **95**, fyy225 (2019).
65. Levy-Booth, D. J. *et al.* Discovery of lignin-transforming bacteria and enzymes in thermophilic environments using stable isotope probing. *ISME. J.* **16**, 1944–1956 (2022).
66. Eiland, F., Klamer, M., Lind, A.-M., Leth, M. & Bååth, E. Influence of initial C/N ratio on chemical and microbial composition during long term composting of straw. *Microb. Ecol.* **41**, 272–280 (2001).
67. Lehmann, M. F., Bernasconi, S. M., Barbieri, A. & McKenzie, J. A. Preservation of organic matter and alteration of its carbon and nitrogen isotope composition during simulated and in situ early sedimentary diagenesis. *Geochim. Cosmochim. Acta.* **66**, 3573–3584 (2002).
68. Meriem, S., Tjitrosoedirjo, S., Kotowska, M. M., Hertel, D. & Triadiati, T. Carbon and nitrogen stocks in dead wood of tropical lowland forests as dependent on wood decay stages and land-use intensity. *Ann. For. Res.* **59**, 299–310 (2016).
69. Tramoy, R., Sebilo, M., Nguyen Tu, T. T. & Schnyder, J. Carbon and nitrogen dynamics in decaying wood: Paleoenvironmental implications. *Environ. Chem.* **14**, 9 (2017).
70. Langmead, B. & Salzberg, S. L. Fast gapped-read alignment with Bowtie 2. *Nat. Methods.* **9**, 357–359 (2012).
71. Chen, S., Zhou, Y., Chen, Y. & Gu, J. fastp: An ultra-fast all-in-one FASTQ preprocessor. *Bioinformatics.* **34**, i884–i890 (2018).
72. Bankevich, A. *et al.* SPAdes: A New genome assembly algorithm and its applications to single-cell sequencing. *J. Comput. Biol.* **19**, 455–477 (2012).
73. Okonechnikov, K., Conesa, A. & García-Alcalde, F. Qualimap 2: Advanced multi-sample quality control for high-throughput sequencing data. *Bioinformatics.* **32**, 292–294 (2016).
74. Parks, D. H., Imelfort, M., Skennerton, C. T., Hugenholtz, P. & Tyson, G. W. CheckM: Assessing the quality of microbial genomes recovered from isolates, single cells, and metagenomes. *Genome. Res.* **25**, 1043–1055 (2015).
75. Seemann, T. Prokka: Rapid prokaryotic genome annotation. *Bioinformatics.* **30**, 2068–2069 (2014).
76. Galata, V., Fehlmann, T., Backes, C. & Keller, A. PLSDb: A resource of complete bacterial plasmids. *Nucleic. Acids. Res.* **47**, D195–D202 (2019).
77. Aziz, R. K. *et al.* The RAST Server: Rapid annotations using subsystems technology. *BMC. Genom.* **9**, 75 (2008).
78. Huerta-Cepas, J. *et al.* eggNOG 4.5: A hierarchical orthology framework with improved functional annotations for eukaryotic, prokaryotic and viral sequences. *Nucleic. Acids. Res.* **44**, D286–293 (2016).
79. Lombard, V., Golaconda Ramulu, H., Drula, E., Coutinho, P. M. & Henriksas, B. The carbohydrate-active enzymes database (CAZY) in 2013. *Nucleic. Acids. Res.* **42**, D490–D495 (2014).
80. Weber, T. *et al.* antiSMASH 3.0—a comprehensive resource for the genome mining of biosynthetic gene clusters. *Nucleic. Acids. Res.* **43**, W237–W243 (2015).
81. Chaumeil, P.-A., Mussig, A. J., Hugenholtz, P. & Parks, D. H. GTDB-Tk: A toolkit to classify genomes with the genome taxonomy database. *Bioinformatics.* **35**, btz848 (2019).
82. Parks, D. H. *et al.* A standardized bacterial taxonomy based on genome phylogeny substantially revises the tree of life. *Nat. Biotechnol.* **36**, 996–1004 (2018).

## Acknowledgements

This work was supported by the Industrial Chair “WinEsca” funded by ANR (French National Research Agency), the JAs Hennessy & Co and the GreenCell companies and the financial support of the E2S-UPPA Project.

## Author contributions

R.H., C.R., A.G., S.C., L.A. performed the experiment. R.H., A.Y., C.R., A.G., A.L., S.C., L.A., G.B. analyzed the data. R.H., C.R., S.C., P.R., G.B. L.A. contributed to the writing of the manuscript. All authors provided critical revision of the manuscript. All authors read and approved the final manuscript.

## Competing interests

The authors declare no competing interests.

## Additional information

**Supplementary Information** The online version contains supplementary material available at <https://doi.org/10.1038/s41598-024-66620-x>.

**Correspondence** and requests for materials should be addressed to R.H.

**Reprints and permissions information** is available at [www.nature.com/reprints](http://www.nature.com/reprints).

**Publisher's note** Springer Nature remains neutral with regard to jurisdictional claims in published maps and institutional affiliations.



**Open Access** This article is licensed under a Creative Commons Attribution 4.0 International License, which permits use, sharing, adaptation, distribution and reproduction in any medium or format, as long as you give appropriate credit to the original author(s) and the source, provide a link to the Creative Commons licence, and indicate if changes were made. The images or other third party material in this article are included in the article's Creative Commons licence, unless indicated otherwise in a credit line to the material. If material is not included in the article's Creative Commons licence and your intended use is not permitted by statutory regulation or exceeds the permitted use, you will need to obtain permission directly from the copyright holder. To view a copy of this licence, visit <http://creativecommons.org/licenses/by/4.0/>.

© The Author(s) 2024